Title
Developing new predictive alarms based on ECG metrics for bradyasystolic cardiac arrest

Journal
Physiological Measurement, 36(12)

ISSN
0967-3334

Authors
Ding, Quan
Bai, Yong
Tinoco, Adelita
et al.

Publication Date
2015-12-01

DOI
10.1088/0967-3334/36/12/2405

Peer reviewed

Published in final edited form as:

Physiol Meas. 2015 December ; 36(12): 2405–2422. doi:10.1088/0967-3334/36/12/2405.

Developing New Predictive Alarms Based on ECG Metrics for Bradyasystolic Cardiac Arrest

Quan Ding[1], **Yong Bai**[2], **Adelita Tinoco**[1], **David Mortara**[1,3], **Duc Do**[5], **Noel G. Boyle**[5], **Michele M. Pelter**[1], and **Xiao Hu**[1,4]

[1]Department of Physiological Nursing, School of Nursing, University of California, San Francisco

[2]Biomedical Engineering Graduate Program, Henry Samueli School of Engineering and Applied Science, University of California, Los Angeles

[3]Mortara Instrument, Milwaukee, WI, USA

[4]Department of Neurosurgery, David Geffen School of Medicine, University of California, Los Angeles

[5]Cardiac Arrhythmia Center, UCLA Health System, David Geffen School of Medicine at UCLA, Los Angeles, CA

Abstract

Objectives—We investigated 17 metrics derived from four leads of electrocardiographic (ECG) signals from hospital patient monitors to develop new ECG alarms for predicting adult bradyasystolic cardiac arrest events.

Methods—A retrospective case-control study was designed to analyze 17 ECG metrics from 27 adult bradyasystolic and 304 control patients. The 17 metrics consisted of PR interval (PR), P-wave duration (Pdur), QRS duration (QRSdur), RR interval (RR), QT interval (QT), estimate of serum K+ using only frontal leads (SerumK2), T-wave complexity (T Complex), ST segment levels for leads I, II, V (ST I, ST II, ST V), and 7 heart rate variability (HRV) metrics. These 7 HRV metrics were standard deviation of normal to normal intervals (SDNN), total power, very low frequency power, low frequency power, high frequency power, normalized low frequency power, and normalized high frequency power. Controls were matched by gender, age (± 5 years), admission to the same hospital unit within the same month, and the same major diagnostic category. A research ECG analysis software program developed by co-author Mortara D was used to automatically extract the metrics. The absolute value for each ECG metric, and the duration, terminal value, and slope of the dominant trend for each ECG metric, were derived and tested as the alarm conditions. The maximal true positive rate (TPR) of detecting cardiac arrest at a prescribed maximal false positive rate (FPR) based on the trending conditions was reported. Lead time was also recorded as the time between the first time alarm condition was triggered and the event of cardiac arrest.

Corresponding Author: Xiao Hu, Ph.D., 2 Koret Way, Nursing, San Francisco, CA 94143, Office (415) 476-4412, FAX: (415) 476-8899, xiao.hu@nursing.ucsf.edu.

Results—While conditions based on the absolute values of ECG metrics do not provide discriminative information to predict bradyasystolic cardiac arrest, the trending conditions can be useful. For example, with a max FPR = 5.0%, some derived alarms conditions are: trend duration of PR > 2.8 hours (TPR = 48.2%, lead time = 10.0 ± 6.6 hours), trend duration of QRSdur > 2.7 hours (TPR = 40.7%, lead time = 8.8 ± 6.2 hours), trend duration of RR > 3.5 hours (TPR = 51.9%, lead time = 6.4 ± 5.5 hours), trend duration of T Complex > 2.9 hours (TPR = 40.7%, lead time = 6.8 ± 5.5 hours), trend duration of ST I > 3.0 hours (TPR of 51.9%, lead time = 8.4 ± 8.0 hours), trend duration of SDNN > 3.6 hours (TPR of 40.7%, lead time = 11.0 ± 8.6 hours), trend duration of HRV total power > 3.0 hours (TPR of 25.9%, lead time = 7.5 ± 8.1 hours), terminal value of ST I < −56 μV (TPR = 22.2%, lead time = 12.8 ± 8.3 hours), and slope of QR > 19.4 ms/hour (TPR = 25.9%, lead time = 6.7 ± 6.9 hours). Eleven trend duration alarms, eight terminal value alarms, and ten slope alarms, achieved a positive TPR with zero FPR. Furthermore, these alarms conditions with zero PFR can be combined by the “OR” logic could further improve the TPR without increasing the FPR.

Conclusions—The trend duration, terminal value, and slope of the dominant trend of the ECG metrics considered in this study are able to predict a subset of patients with bradyasystolic cardiac arrests with low or even zero FPR, which can be used for developing new ECG alarms.

1. INTRODUCTION

Patient monitors with alarm systems are essential diagnostic devices providing continuous display and interpretation of patients’ vital functions. Despite their wide usage among hospital care units, alarm fatigue problems occur when the number of alarms overwhelms nurses and physicians, causing alarms to be disabled or ignored, which may lead to serious injuries and even death (Bell, 2010, Kenny, 2011, The Joint Commission, 2013, Borowski et al., 2011). It is estimated that the number of alarms per patient per day can reach several hundred (The Joint Commission, 2013), 80% - 99% of which are false positives and/or clinically insignificant and do not require clinical intervention (Lawless, 1994, Chambrin et al., 1999, Drew et al., 2014). Alarm fatigue is ranked by hospitals as the top patient safety concern according to a recent survey (Mabuyi, 2013) and in 2014, the Joint Commission added alarm management as a National Patient Safety.

To tackle the alarm fatigue problems, many studies have focused on reducing the false alarm rate for certain alarms. Aboukhalil et al. showed that false electrocardiography (ECG) arrhythmia alarms could be suppressed by also using arterial blood pressure (ABP) signal and signal quality indices (Aboukhalil et al., 2008). Deshmane used pulse oximetry or photoplethysmogram (PPG) in addition to ABP and ECG signals to suppress false ECG critical arrhythmia alarms (Deshmane, 2009). Observing the fact that the ventricular tachycardia (VT) alarms had relatively high true alarm reduction rates but with low false alarm reduction rate in both studies, Li and Clifford developed a data fusion scheme using features extracted from the ECG, ABP and PPG to reduce false arrhythmia alarms, achieving a false alarm reduction rate of 30% and a true alarm reduction rate below 1% (Li and Clifford, 2012). More recently, Salas-Boni et al. used the discrete wavelet transform and L1-regularized logistic regression classifier to achieve a false alarm reduction rate of 21% for the MIMIC II dataset (Saeed et al., 2011) and a false alarm reduction rate of 36% for a

UCSF dataset (Drew et al., 2014), both with zero true alarm reduction rate (Salas-Boni et al., 2014).

On the other hand, it is believed that alarm fatigue reflects a more general data-overloading problem in healthcare, which can be potentially addressed using precise predictive models developed using modern machine learning techniques and big healthcare dataset. To this end, efforts, in particular, have been made to develop predictive models to detect patient deterioration or subacute patient illness in critical care settings, since predictions of catastrophic clinical events will not only reduce false alarms but also improve management of hospitalized patients. Escobar et al. developed a predictive model using electronic medical record (EMR) data to predict unplanned transfers from medical-surgical wards to intensive care units (Escobar et al., 2012). Moorman et al. showed that heart rate characteristics are clinically useful in early detection of neonatal sepsis and can reduce the mortality rate in very low birth weight infants (Moorman et al., 2011a, Moorman et al., 2011b). Hu et al. discovered combinations of individual monitor alarms, known as SuperAlarm, to predict impending code blue (CB) events, which were defined as cardiac arrests with loss of central pulse, apnea, and unresponsiveness (Hu et al., 2012). The SuperAlarm framework automatically searches alarm combination patterns that provide distinctive information between the case patients and their controls. With less emphasis on individual alarms, the framework is less sensitive to false alarms. Bai et al. further integrated laboratory test results with existing monitor alarms in the SuperAlarm framework to improve prediction performance (Bai et al., 2014). Hu et al. also derived additional alarms based on ECG metrics currently not available on patient monitors (Hu et al., 2013), which could be further incorporated into the SuperAlarm framework as a possible solution to improve cardiac patient monitoring. The ECG analysis method proposed by Hu (Hu et al., 2013) was labor intensive because manual inspection to ensure correct detection of P wave, T wave, and QRS onset/offset were performed. Consequently, with a dataset of 22 cases and their 300 controls, only the 22 cases and 45 of the controls were analyzed.

In this study, we increased the number of case patients to 27 by considering more bradyasystolic cardiac arrest patients from the UCSF dataset (Drew et al., 2014) and the number of matched control patients increased to 304. Our ultimate goal is to identify predictive metrics that can be extracted from ECG waveform and integrate them using SuperAlarm framework. However, to robustly identify those metrics, it is imperative that the preliminary analysis in our previous work be expanded to include all control patients. To leverage decades of research in ECG analysis and avoid re-implementing ECG analysis methods as done in our previous work, a research ECG analysis software program written by co-author Mortara D is used for ECG analysis in the present study. ECG analysis algorithms implemented in this research software are indeed used in many commercial lines of FDA-approved ECG monitoring software from Mortara Instrument (Milwaukee, WI). This research software has also been used for ECG analysis in several other studies (Pickham et al., 2012, He et al., 2011, Liao et al., 2011). Using this software enabled us to analyze all the available ECG recordings, and still focus on analyzing the predictive power of ECG metrics and their trending patterns for bradyasystolic cardiac arrest. The adopted ECG analysis program automatically calculates various ECG metrics from the waveform data and generates the results in comma-separated values (CSV) files, which can be easily extracted.

With the efficiency of the ECG analysis program, we were able to analyze data from all the 27 cases and 304 controls. Furthermore, physiological underpinnings of these ECG metrics are all well-understood and can be readily interpreted by clinicians offering advantages over those metrics purely driven by statistical analysis alone. Because this program also outputs the waveform of the processed ECG beat and the detected locations of P, QRS, and T waves, we were able to evaluate the accuracy of this program in detecting these ECG landmarks. This analysis is necessary because all the downstream analysis will be affected by the accuracy of P-QRS-T wave detection.

A further innovation in the present study was the development of a new algorithm to identify dominant trending patterns in a time series of ECG metrics. Our motivation to develop this trending algorithm is that we expect additional predictive information can be extracted from inspecting the changes of ECG metrics instead of only relying on the absolute values. After robustly identifying a trending pattern, we were able to use the same case-control design in our previous work (Hu et al., 2013) to examine the predictive power of the characteristics of the identified trending.

2. METHODS

2.1 Patient Data

Continuous waveforms of four ECG leads (I, II, III, and V), all sampled at 240 Hz, were compiled using the BedMaster system (Excel Medical Electronics, Jupiter, FL), which archives continuous waveform data from General Electric bedside monitors (GE Healthcare, Waukesha, WI) throughout our hospital's acute care units in both University of California, Los Angeles (UCLA) and University of California, San Francisco (UCSF). This study received approval from the Institutional Review Board at UCLA and the Committee on Human Research at UCSF.

Patients with age ≥ 18 years and at least 3 consecutive hours of monitoring data prior to a CB call due to bradyasystolic cardiac arrest were selected from a pool of CB patients as the cases. This pool consists of patients with CB events between April 2010 and March 2012 at UCLA and in March 2013 at UCSF. For the cases with more than one CB, only the initial CB call was included in the analysis. Then for each case, we extracted signals for up to 24 hours prior to the code call. We selected control patients by matching for (1) gender, (2) age (± 5 years), (3) admission to same hospital unit within the same month, and (4) same major diagnostic category. A total of 27 case patients and 304 control patients were selected.

2.2 ECG Metrics

17 ECG metrics automatically generated by the ECG analysis program analyzed in this study were:

- PR interval (PR), interval from P onset to QRS onset in milliseconds.
- P-wave duration (Pdur), interval from P onset to P offset in milliseconds.
- QRS duration (QRSdur), interval from QRS onset to QRS offset in milliseconds.
- RR interval (RR), interval from R peak to R peak in milliseconds.

- QT interval (QT), interval from QRS onset to T offset in milliseconds.
- Estimate of blood potassium using only frontal leads (SerumK2), derived from a ratio of the T wave slope and amplitude (Corsi et al., 2012).
- T-wave complexity (T Complex), the square root of the ratio of the 2nd to 1st eigenvalues of the spatial covariance matrix obtained from samples in the extended STT interval of each QRST complex. (Priori et al., 1997).
- ST segment levels for leads I, II, V (ST I, ST II, ST V), relative amplitudes of the J (QRS offset) + 60ms point compared to QRS onset in millivolts.
- Standard deviation of normal to normal intervals (SDNN) in milliseconds.
- Heart rate variability (HRV) total power (<0.4Hz) in millisecond^2.
- HRV very low frequency power (VLF) (0.003-0.04 Hz) in millisecond^2.
- HRV low frequency power (LF) (0.04-0.15Hz) in millisecond^2.
- HRV high frequency power (HF) (0.15-0.4Hz) in millisecond^2.
- HRV normalized low frequency power (norm LF) in %.
- HRV normalized high frequency power (norm HF) in %.

The metrics were determined globally based on the absolute spatial velocity (ASV), the sum of absolute sample differences over the available leads from each 5-minute window. Successive windows were overlapped by 4 minutes, and therefore the metrics were generated every 1 minute.

2.3 Quality Control Assessment of the ECG Analysis Program

Since all the 17 ECG metrics considered in this paper depend on onsets and offsets of P, QRS, and T waves, the accuracy of detecting these onsets and offsets is of great importance in our study. In order to evaluate the quality of the ECG analysis program, we randomly selected two 5-minute windows from each patient, resulting in a total of 662 windows. For each window, the average beat waveform as well as detected P onset, P offset, QRS onset, QRS offset, T offset, were extracted and plotted. A clinician then visually inspected all the plots and manually recorded if the onsets and offsets had been correctly identified. To ensure inter-rater reliability, another clinician did the same inspection on a random subset of 10% of the 662 plots (66 plots). The annotations on this subset from the two clinicians were compared to validate the reliability of the first clinician. Finally, the accuracy of each onset or offset detection from the first clinician was reported as the quality control assessment of the ECG analysis program.

2.4 Preprocessing

A median filter was used to preprocess the ECG metrics, which replaced the current metric by the median of the most recent 2k+1 metrics. This preprocessing filter is popular for reducing artifacts or outliers without attenuating the signal quality (Mäkivirta et al., 1991). A delay of k samples was introduced by the median filter, and in our case, the delay was k minutes. Larger k enables the filter to remove outliers in a longer duration, but increases the

risk of losing signal details. k = 4, which corresponded to a median filter with length of 9 minutes, was selected in this study because it had a reasonable tradeoff between outlier suppression and loss of signal details.

2.5 Trending Analysis

It is hypothesized that the trending characteristics of ECG metrics provide certain discriminative information about the CB patients and their controls. Therefore, we developed a multi-scale approach to find the dominant trend, i.e., the longest monotonically increasing or decreasing duration for each metric. Once the dominant trend was determined, we could easily find its duration, terminal value, and slope as depicted in Figure 1, where the slope was derived by a robust linear fitting algorithm (Hadi and Simonoff, 1993). Next, we will describe how the dominant trend is determined by the multi-scale approach.

If a function is monotonically increasing or decreasing on a window, it must be monotonic on any sub-windows. If we used linear fitting on any sub-windows, the slope sign should be the same. In our problem, the ECG metrics could be noisy or disturbed by outliers. As a result, the slope sign may be different for certain sub-windows, even if the trending is visually obvious. Therefore, it was impractical to require the slope sign be the same for any sub-window. Instead, we required the slope sign be the same for a set of overlapped sub-windows which covered the range of the window being examined. If the sub-window length is small, the linear fitting is sensitive to outliers, and the slope sign can be easily affected by outliers. On the other hand, if the sub-window length is large, linear fitting is less sensitive to outliers, but it may smooth the real trending pattern. In this study, we proposed a multi-scale approach to automatically select the optimal length of the sub-windows.

We allowed the sub-window length to range from 10 minutes to 1 hour with a step size of 1 minute. Then for each value of the sub-window length, a set of overlapping sub-windows was created from the start of recording to the end with a sub-window increment of 1 minute. The robust linear fitting (Hadi and Simonoff, 1993) was performed on each sub-window and the slope signs were recorded. The percentage of + and - slope signs were calculated. The sign with a larger percentage was called the dominant slope sign. Note that we had obtained percentage of slope signs for each sub-window length. Then optimal sub-window length corresponded to the largest percentage of the dominant slope sign. Finally, the dominant trend was the interval that had the most number of consecutive dominant slope signs for the optimal sub-window length. An example is shown in Figure 2 to illustrate the procedure.

2.6 Statistical Analysis

In this study, we focused on developing new alarms based on each individual ECG metric and an “OR” logic to combine individual alarms. Because the cause of bradyasystolic cardiac arrest can be different, we do not expect a single metric or a simple combination of metrics can achieve high sensitivities. Therefore, we focused on the best true positive rate (TPR) achievable with a user-prescribed maximal false positive rate (FPR). This allowed us to evaluate the predictivity provided by each metric. As mentioned previously, our goal is to integrate these new ECG alarms into the SuperAlarm scheme, which can generate more

complicated and meaningful combinations of individual alarms as a possible solution to the alarm fatigue problems.

We first estimated the distributions of the absolute values of the ECG metrics and examined if they provide predictive information of the CB events. Then we derived the duration, terminal value, and slope of the dominant trend, of the ECG metrics and studied their predictive power of the CB events. A detailed description on the dominant trend and how we derived it is presented in the next subsection.

These three parameters based on the dominant trend allow us to develop three trend alarms: trend duration alarm, terminal value alarm, and slope alarm. We specified a maximal FPR for trend alarm to determine a threshold so that percentage of control patients with a trending parameter larger than this threshold could not be greater than this maximal FPR. For the terminal value alarm and the slope alarm, both upper and lower thresholds were tested, while for the trend duration alarm, only an upper threshold was tested. This is because it only makes sense to trigger an alarm when the trend duration is greater than a certain threshold. We recorded the TPR that could be obtained using this trend alarm. The TPR achievable with the maximal FPR was reported, as well as the corresponding threshold value as the alarm condition. We also reported the lead time of each alarm condition as the time between the first time alarm condition was triggered and the event of cardiac arrest.

3. RESULTS

The patient characteristics of both case and control groups are summarized in Table 1. While 66.7% of the case patients were male, 72.4% of the control patients were male. The average ages of the case and control patients were 61.4 and 63.2 years, respectively. Most arrests were caused by multi-organ failure (44.4%), followed by respiratory failture (25.9%). Sinus arrest (37.0%) was the major arrest subtype, followed by complete heart block 7 (25.9%).

When evaluating the quality of the ECG analysis program, the P onset, P offset and T offset detection was considered as correct when there was a discernible P or T wave and the program correctly identifies the landmark or when P or T wave was indiscernible and the program was not detecting the P or T wave. By comparing annotations on the subset from the two clinicians, there was 98.5% (65/66) agreement as to whether their annotations were the same for each plot. This served as evidence that the first clinician was reliable in annotating the onset/offset detection. The first clinician's annotations show that the ECG analysis program has correctly identified 85.0% of P onsets, 86.9% of P offsets, 97.0% of QRS onsets, 98.2% of QRS offsets, and 87.3% of T offsets.

Fig. 3 compares the distributions of 17 different ECG metrics from the case and control groups. It can be observed that the tail distributions from the case and control groups are very similar. This implies that thresholding the metrics with a small maximal FPR does not provide discriminative information to predict bradyasystolic cardiac arrest.

Table 2 summarizes the true positive rates achievable under the requirement of a prescribed maximal FPR for the upper threshold condition of the dominant trend duration of each ECG metric. Eleven trend duration alarms achieved a positive TPR with zero FPR. The trend

duration alarms based on PR, QRSdur, RR, SDNN, and HRV total, achieved a TPR of 11.1%, while the trend duration alarm based on ST I achieved a TPR of 14.8%, all with zero FPR.

Tables 3 and 4 are similar to Table 2 except that the triggered conditions were based on the upper and lower thresholds of terminal value and slope of each ECG metric, respectively. Eight terminal value alarms and ten slope alarms achieved a positive TPR with zero FPR. Furthermore, new alarms could be developed by combining those zero-FPR alarm conditions of multiple ECG metrics using the “OR” logic to improve the TPR without increasing the FPR. The highest achievable TPRs with zero FPR by performing the “OR” logic on 2, 3, and 4 zero-FPR alarm conditions are reported in Table 5. Note that the combined alarm conditions with the highest achievable TPR (22.2%, 29.6% and 33.3% for 2, 3 and 4 zero-FPR alarm conditions, respectively) happened to be all based on the trend duration alarms.

4. Discussion

In this case-control study, we study the predictive power of 17 ECG metrics for identifying bradyasystolic cardiac arrest. These 17 ECG metrics are PR interval, P-wave duration, QRS duration, RR interval, QT interval, estimate of serum K+ using only frontal leads, T-wave complexity, ST segment levels for leads I, II, V, standard deviation of normal to normal intervals, HRV total power, HRV very low frequency power, HRV low frequency power, HRV high frequency power, HRV normalized low frequency power, and HRV normalized high frequency power. The extraction of ECG metrics is automatically done by a research ECG analysis program, which has a high accuracy of identifying ECG landmarks. We first analyze the distribution of each ECG metric from the case and control groups, and observe that the absolute values do not provide much predictive information, which is contrary to the results in our prior study (Hu et al., 2013). This may be because the previous study only had 22 case patients and 45 control patients, which may not have been a representative sample. In this study, we increase the number of patients to 27 cases and 304 controls, which would be expected to be more representative.

Next, the dominant trend for each ECG metric needs to be detected in order to derive the trend parameters for statistical analysis. While there exist many trend detection methods such as robust linear fitting (Hu et al., 2013), fuzzy logic course approach (Steimann, 1995), noise-rejection fuzzy C-means clustering (Melek et al., 2005), Trigg's statistical approach (Hope et al., 1973), wavelet-based approach (Konstantinov and Yoshida, 1992), they are all based on a prescribed sub-window length. However, using a prescribed sub-window length may not work for all patients. This is because different patients may have different levels of outlier and trending patterns and the optimal sub-window length is patient-dependent. Therefore, we propose a multi-scale approach to automatically determine the optimal sub-window length from the largest percentage of the dominant slope sign and use it to detect the dominant trend. Furthermore, our approach does not require prescribed thresholds or trend templates, making it more robust than other existing approaches such as cumulative sum (CUMSUM) (Charbonnier et al., 2004) and TrenDx (Haimowitz et al., 1995).

Once the dominant trend is determined, the corresponding trend duration, terminal value and slope are derived from the dominant trend and tested as alarm conditions. We report the achievable TPRs with prescribed maximal FPRs. Our results show that the trending of a single ECG metric has certain predictive power and can achieve up to a TPR of 14.8% (trend duration alarm of ST I) with zero FPR or a TPR of 51.9% (trend duration alarm of RR or ST I) with a maximal FPR of 5.0%. The 'OR' logic combination of 4 single-metric alarm conditions can achieve a TPR of 33.3% with zero FPR. However, we should not implement the new alarms directly in a clinical setting since they do not reduce existing false alarms and therefore cannot alleviate the alarm fatigue problem. Rather, we expect to integrate the new alarms into the SuperAlarm framework because we anticipate the combination of metrics to identify patients at risk for cardiac arrest has the potential to reduce false positive alarms. A recent study that integrates laboratory test results with existing monitor alarms in the SuperAlarm framework improved the accuracy of code blue event prediction (Bai et al., 2014). This study indicates that SuperAlarm has the potential to incorporate multi-domain clinical data for improved patient monitoring and possibly reduction of false alarms. Therefore, the new ECG alarms derived in this study can be integrated into SuperAlarm and provide more predictive information in the ECG trend domain. This will be the focus in a future study to determine its accuracy and potential impact on clinical outcomes.

While this study has developed a novel method to analyze the predictive power of ECG metrics and derive new alarms, it still has some limitations. First, the ECG metrics studied in this paper do not include ECG amplitudes except ST segment levels. Additional metrics characterizing ECG amplitudes may provide more predictive information of bradyasystolic or other cardiac arrest and heart failure (Hu et al., 2013, Ostman-Smith et al., 2010, Kataoka and Madias, 2011, Madias, 2009). The 7 HRV metrics are standard ones. They do not include more recent metrics such as asymmetry, entropy, or non-stationarity, which may provide additional information as well (Moorman et al., 2011a, Moorman et al., 2011b). In addition, no logic is implemented to determine whether a detected dominant trend is valid. This is because the dominant trend is sometimes corrupted by outliers and artifacts, and therefore is difficult to observe. Without ground truth of the dominant trend, the reported TPRs may be overestimated as the derived duration, terminal value and slope may not be from the correct trend. Finally, only patients with bradyasystolic cardiac arrest are considered in this study. If we study a different type of cardiac arrest, it is likely that the same ECG metrics may not be identified, given the different pathophysiologic mechanisms of cardiac arrest. Bradyasystolic arrests are primarily seen in patients with multiorgan failure where the bradycardia is reflective of conduction dysfunction from metabolic derangements and for which PR interval and QRS duration prolongation is a reflection of these abnormalities, and in respiratory failure where bradycardia is a result of intrinsic cardiac release of adenosine as a protective mechanism against hypoxia (Belardinelli et al., 1980, Senges et al., 1979, Mustafa et al., 2009). ST segment changes, however, which represent cardiac ischemia can be a result of many different processes and are likely not as specific to bradyasystolic arrests (Attin et al., 2014).

5. Conclusion

We report a case-control study that develops new predictive alarms for bradyasystolic cardiac arrest based on ECG Metrics. Results show that the distributions of each ECG metric from the case and control groups are very similar and therefore the absolute value of each ECG metric does not provide much predictive information. A multi-scale approach is proposed to detect the dominant trend of each ECG metric and the corresponding duration, terminal value, and slope of the dominant trend are derived and tested as alarm conditions. Results show that these trending parameters provide certain discriminative information of bradyasystolic cardiac arrest with hours of lead time. These new alarms have the potential to be incorporated into the SuperAlarm framework to greatly improve the accuracy of predictive alarm systems.

Acknowledgments

This work was partially supported by the UCSF Middle Career Scientist Award, UCSF Institute for Computational Health Sciences, AHRQ grant 1R18H5022860-01A1, and R01HL128679-01.

REFERENCES

ABOUKHALIL A, NIELSEN L, SAEED M, MARK RG, CLIFFORD GD. Reducing false alarm rates for critical arrhythmias using the arterial blood pressure waveform. J Biomed Inform. 2008; 41:442–51. [PubMed: 18440873]

ATTIN M, FELD G, LEMUS H, NAJARIAN K, SHANDILYA S, WANG L, SABOURIAZAD P, LIN CD. Electrocardiogram characteristics prior to inhospital cardiac arrest. J Clin Monit Comput. 2014

BAI Y, DO DH, HARRIS PRE, SCHINDLER D, BOYLE NG, DREW BJ, HU X. Integrating monitor alarms with laboratory test results to enhance patient deterioration prediction. Journal of biomedical informatics. 2014; 53:81–92. [PubMed: 25240252]

BELARDINELLI L, BELLONI FL, RUBIO R, BERNE RM. Atrioventricular conduction disturbances during hypoxia. Possible role of adenosine in rabbit and guinea pig heart. Circ Res. 1980; 47:684–91. [PubMed: 7418128]

BELL L. Alarm fatigue linked to patient's death. Interview by Laura Wallis. Am J Nurs. 2010; 110:16. [PubMed: 20574186]

BOROWSKI M, GORGES M, FRIED R, SUCH O, WREDE C, IMHOFF M. Medical device alarms. Biomed Tech (Berl). 2011; 56:73–83. [PubMed: 21366502]

CHAMBRIN MC, RAVAUX P, CALVELO-AROS D, JABORSKA A, CHOPIN C, BONIFACE B. Multicentric study of monitoring alarms in the adult intensive care unit (ICU): a descriptive analysis. Intensive Care Med. 1999; 25:1360–6. [PubMed: 10660842]

CHARBONNIER S, BECQ G, BIOT L. On-line segmentation algorithm for continuously monitored data in intensive care units. Biomedical Engineering, IEEE Transactions on. 2004; 51:484–492.

CORSI, C.; DEBIE, J.; NAPOLITANO, C.; PRIORI, S.; MORTARA, D.; SEVERI, S. Computing in Cardiology (CinC). Vol. 2012. IEEE; 2012. Validation of a Novel Method for Non-invasive Blood Potassium Quantification from the ECG.; p. 105-108.

DESHMANE, AV. False arrhythmia alarm suppression using ECG, ABP, and photoplethysmogram. Massachusetts Institute of Technology; 2009.

DREW BJ, HARRIS P, ZÈGRE-HEMSEY JK, MAMMONE T, SCHINDLER D, SALASBONI R, BAI Y, TINOCO A, DING Q, HU X. Insights into the Problem of Alarm Fatigue with Physiologic Monitor Devices: A Comprehensive Observational Study of Consecutive Intensive Care Unit Patients. PloS one. 2014; 9:e110274. [PubMed: 25338067]

ESCOBAR GJ, LAGUARDIA JC, TURK BJ, RAGINS A, KIPNIS P, DRAPER D. Early detection of impending physiologic deterioration among patients who are not in intensive care: development of

predictive models using data from an automated electronic medical record. J Hosp Med. 2012; 7:388–95. [PubMed: 22447632]

HADI AS, SIMONOFF JS. Procedures for the identification of multiple outliers in linear models. Journal of the American Statistical Association. 1993; 88:1264–1272.

HAIMOWITZ IJ, LE PP, KOHANE IS. Clinical monitoring using regression-based trend templates. Artificial intelligence in medicine. 1995; 7:473–496. [PubMed: 8963372]

HE F, SHAFFER ML, LI X, RODRIGUEZ-COLON S, WOLBRETTE DL, WILLIAMS R, CASCIO WE, LIAO D. Individual-level PM2.5 exposure and the time course of impaired heart rate variability: the APACR Study. J Expo Sci Environ Epidemiol. 2011; 21:65–73. [PubMed: 20372190]

HOPE CE, LEWIS CD, PERRY IR, GAMBLE A. Computed trend analysis in automated patient monitoring systems. Br J Anaesth. 1973; 45:440–9. [PubMed: 4123708]

HU X, DO D, BAI Y, BOYLE NG. A case-control study of non-monitored ECG metrics preceding in-hospital bradyasystolic cardiac arrest: implication for predictive monitor alarms. J Electrocardiol. 2013; 46:608–15. [PubMed: 24034301]

HU X, SAPO M, NENOV V, BARRY T, KIM S, DO DH, BOYLE N, MARTIN N. Predictive combinations of monitor alarms preceding in-hospital code blue events. J Biomed Inform. 2012; 45:913–21. [PubMed: 22465785]

KATAOKA H, MADIAS JE. Changes in the amplitude of electrocardiogram QRS complexes during follow-up of heart failure patients. J Electrocardiol. 2011; 44:394, e1–9. [PubMed: 21376341]

KENNY PE. Alarm fatigue and patient safety. Pa Nurse. 2011; 66:3, 22.

KONSTANTINOV KB, YOSHIDA T. Real - time qualitative analysis of the temporal shapes of (bio) process variables. AIChE Journal. 1992; 38:1703–1715.

LAWLESS ST. Crying wolf: false alarms in a pediatric intensive care unit. Crit Care Med. 1994; 22:981–5. [PubMed: 8205831]

LI Q, CLIFFORD GD. Signal quality and data fusion for false alarm reduction in the intensive care unit. J Electrocardiol. 2012; 45:596–603. [PubMed: 22960167]

LIAO D, SHAFFER ML, HE F, RODRIGUEZ-COLON S, WU R, WHITSEL EA, BIXLER EO, CASCIO WE. Fine particulate air pollution is associated with higher vulnerability to atrial fibrillation—The APACR study. Journal of Toxicology and Environmental Health, Part A. 2011; 74:693–705. [PubMed: 21480044]

MABUYI, A. First National Survey of Patient-Controlled Analgesia Practices.. SASM Annual Conference; 2013.

MADIAS JE. Mechanism of attenuation of the QRS voltage in heart failure: a hypothesis. Europace. 2009; 11:995–1000. [PubMed: 19493912]

MÄKIVIRTA A, KOSKI E, KARI A, SUKUVAARA T. The median filter as a preprocessor for a patient monitor limit alarm system in intensive care. Computer methods and programs in biomedicine. 1991; 34:139–144. [PubMed: 2060287]

MELEK WW, LU Z, KAPPS A, FRASER WD. Comparison of trend detection algorithms in the analysis of physiological time-series data. Biomedical Engineering, IEEE Transactions on. 2005; 52:639–651.

MOORMAN JR, CARLO WA, KATTWINKEL J, SCHELONKA RL, PORCELLI PJ, NAVARRETE CT, BANCALARI E, ASCHNER JL, WALKER MW, PEREZ JA. Mortality reduction by heart rate characteristic monitoring in very low birth weight neonates: a randomized trial. The Journal of pediatrics. 2011a; 159:900–906. e1. [PubMed: 21864846]

MOORMAN JR, DELOS JB, FLOWER AA, CAO H, KOVATCHEV BP, RICHMAN JS, LAKE DE. Cardiovascular oscillations at the bedside: early diagnosis of neonatal sepsis using heart rate characteristics monitoring. Physiological measurement. 2011b; 32:1821. [PubMed: 22026974]

MUSTAFA SJ, MORRISON RR, TENG B, PELLEG A. Adenosine receptors and the heart: role in regulation of coronary blood flow and cardiac electrophysiology. Handb Exp Pharmacol. 2009:161–88. [PubMed: 19639282]

OSTMAN-SMITH I, WISTEN A, NYLANDER E, BRATT EL, GRANELLI A, OULHAJ A, LJUNGSTROM E. Electrocardiographic amplitudes: a new risk factor for sudden death in hypertrophic cardiomyopathy. Eur Heart J. 2010; 31:439–49. [PubMed: 19897498]

PICKHAM D, MORTARA D, DREW BJ. Time dependent history improves QT interval estimation in atrial fibrillation. J Electrocardiol. 2012; 45:556–60. [PubMed: 23040546]

PRIORI SG, MORTARA DW, NAPOLITANO C, DIEHL L, PAGANINI V, CANTÙ F, CANTÙ G, SCHWARTZ PJ. Evaluation of the spatial aspects of T-wave complexity in the long-QT syndrome. Circulation. 1997; 96:3006–3012. [PubMed: 9386169]

SAEED M, VILLARROEL M, REISNER AT, CLIFFORD G, LEHMAN L-W, MOODY G, HELDT T, KYAW TH, MOODY B, MARK RG. Multiparameter Intelligent Monitoring in Intensive Care II (MIMIC-II): a public-access intensive care unit database. Critical care medicine. 2011; 39:952. [PubMed: 21283005]

SALAS-BONI R, BAI Y, HARRIS PR, DREW BJ, HU X. False ventricular tachycardia alarm suppression in the ICU based on the discrete wavelet transform in the ECG signal. J Electrocardiol. 2014; 47:775–80. [PubMed: 25172188]

SENGES J, MIZUTANI T, PELZER D, BRACHMANN J, SONNHOF U, KUBLER W. Effect of hypoxia on the sinoatrial node, atrium, and atrioventricular node in the rabbit heart. Circ Res. 1979; 44:856–63. [PubMed: 428078]

STEIMANN, F. Diagnostic monitoring of clinical time series. Technische Universität Wien; 1995.

THE JOINT COMMISSION. Medical device alarm safety in hospitals. Sentinel Event Alert. 2013:1–3.

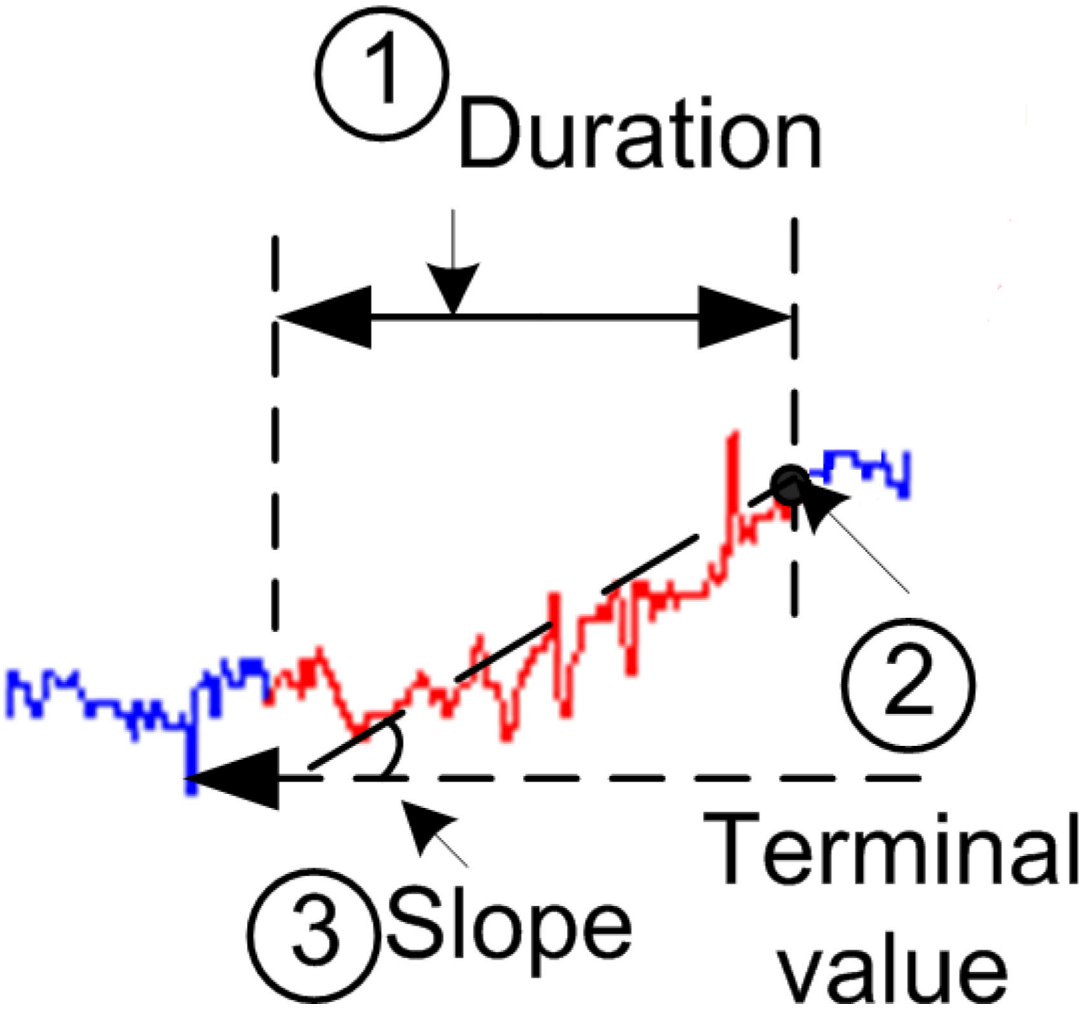

Figure 1.
Duration, terminal value, and slope of the dominant trend. The red color represents the detected dominant trend while the blue color represents the time series of an ECG metric.

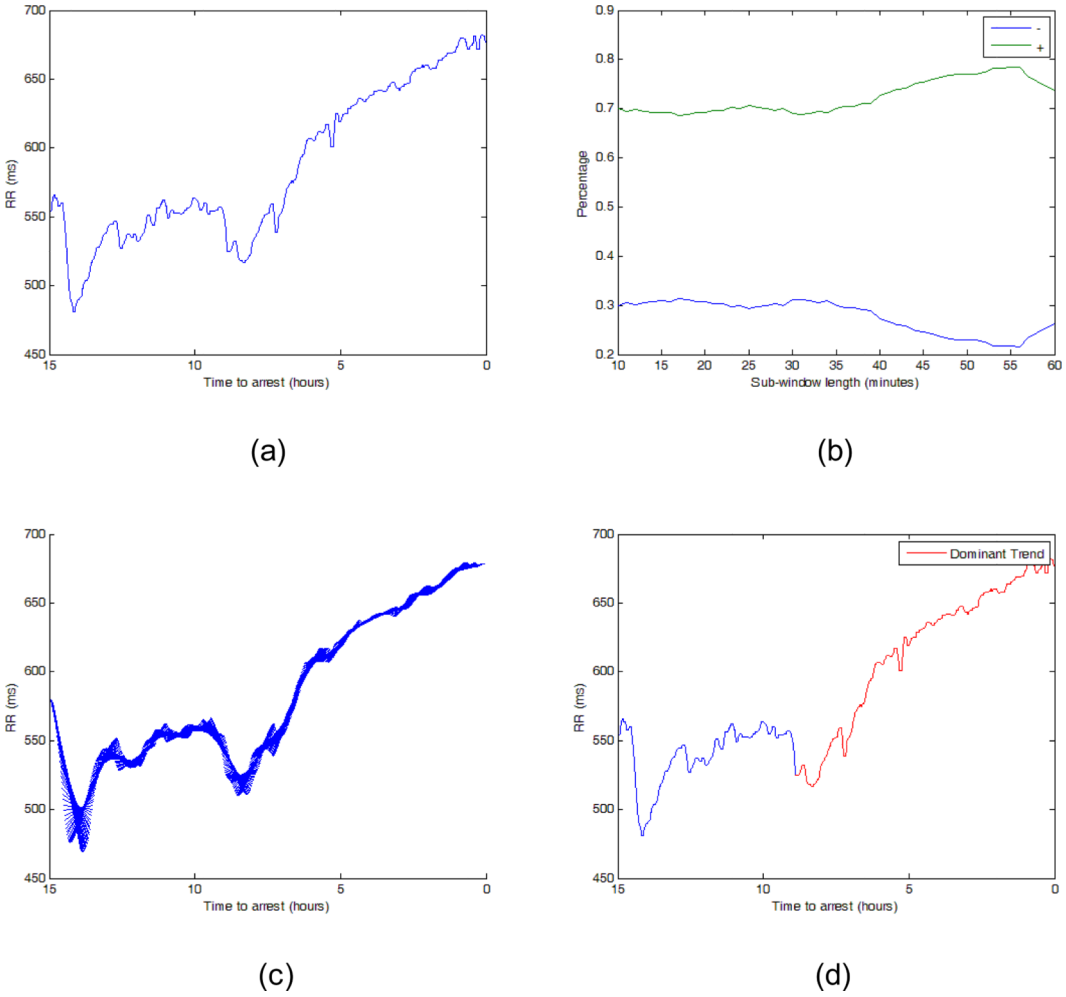

Figure 2.

An example of the multi-scale approach to detect the dominant trending or the longest monotonic window. (a) RR interval for a case patient. (b) Percentage of slope signs vs sub-window length. (c) Robust linear fitting of overlapped sub-windows for the optimal sub-window length. (d) Detected dominant trending.

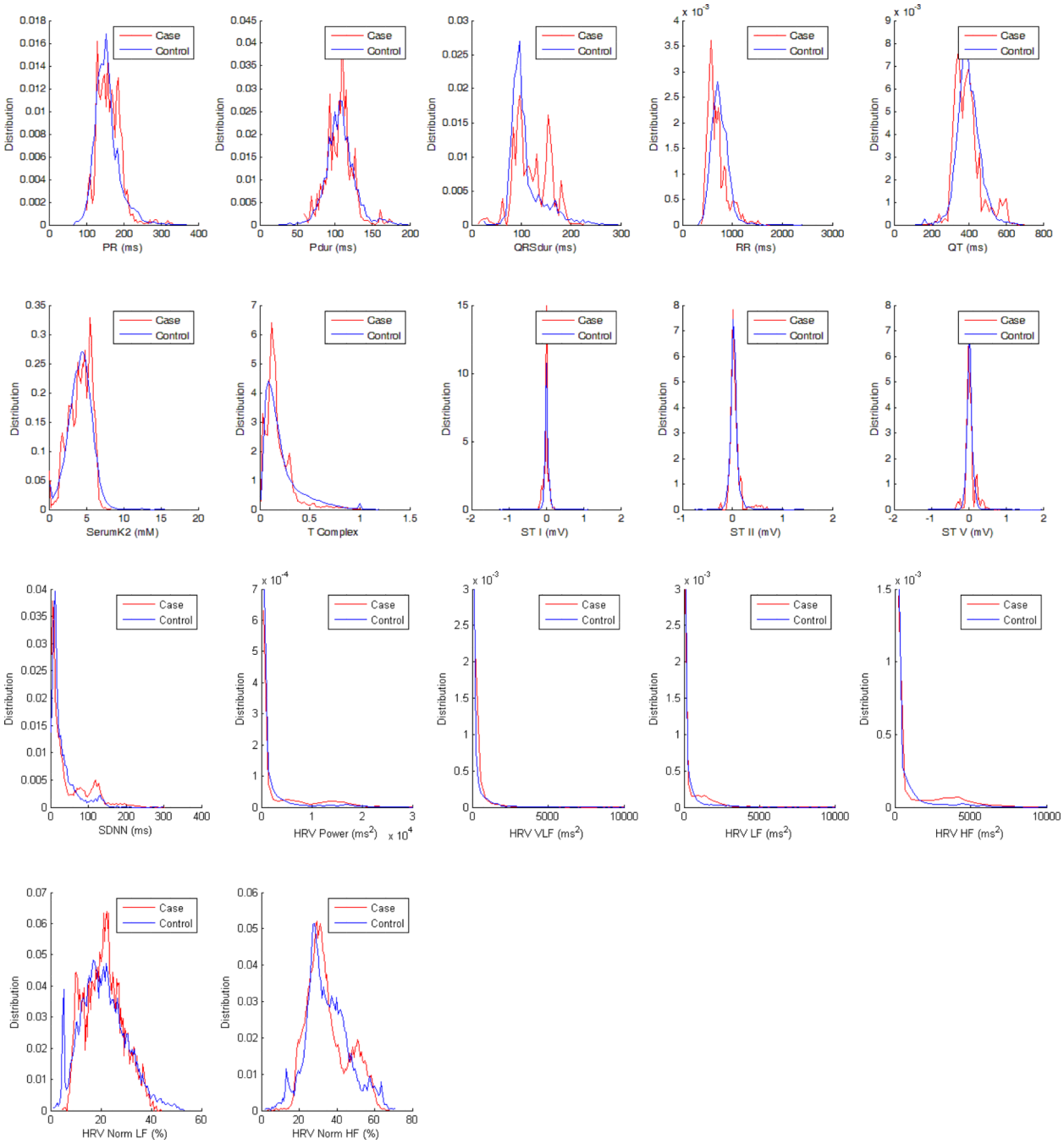

Figure 3.

Comparison of the distributions of 17 ECG metrics from all 27 cardiac arrest patients and control subjects.

Table 1

Patient characteristics of case and control groups.

		Brady Cardiac Arrests	Control
Number of patients		27	304
Male (%)		18 (66.7%)	220 (72.4%)
Age (mean ± SD)		61.4 ± 20.7	63.2 ± 11.8
Total duration of ECG analyzed (hours)		19.4 ± 7.0	22.8 ± 4.1
Causes of arrest (%)	Multi-organ failure	12 (44.4%)	Not applicable
	Respiratory failure	7 (25.9%)	
	Cardiac failure	1 (3.7%)	
	Drug-induced	1 (3.7%)	
	Vagally mediated asystolic event, occurring during the turning of a patient	1 (3.7%)	
	Unknown by documentation	5 (18.5%)	
Arrest subtypes (%)	Sinus arrest	10 (37.0%)	Not applicable
	Complete heart block	7 (25.9%)	
	High-degree AV block	4 (14.8%)	
	Sinus bradycardia	1 (3.7%)	
	Unknown by documentation	5 (18.5%)	

Table 2

List of true positive rate (TPR) achievable under a prescribed maximal false positive rate (FPR) for the trend duration alarm of each ECG metric (27 case patients).

	max FPR = 0.00			max FPR = 0.01			max FPR = 0.05		
	TPR	**Threshold (hours)**	**Lead Time (hours)**	**TPR**	**Threshold (hours)**	**Lead Time (hours)**	**TPR**	**Threshold (hours)**	**Lead Time (hours)**
PR	**11.1%**	**4.4**	**5.0 ± 8.3**	**18.5%**	**3.5**	**8.9 ± 8.0**	**48.2%**	**2.8**	**10.0 ± 6.6**
Pdur	0.0%	4.1	NA	7.4%	3.4	4.5 ± 5.9	25.9%	2.7	6.3 ± 5.3
QRSdur	**11.1%**	**4.1**	**6.7 ± 6.6**	**18.5%**	**3.6**	**5.4 ± 5.0**	**40.7%**	**2.7**	**8.8 ± 6.2**
RR	**11.1%**	**6.5**	**3.6 ± 4.8**	**25.9%**	**5.3**	**6.6 ± 6.1**	**51.9%**	**3.5**	**6.4 ± 5.5**
QT	0.0%	5.6	NA	11.1%	4.2	2.4 ± 0.8	33.3%	3.3	7.0 ± 6.8
SerumK2	7.4%	4.2	4.6 ± 5.3	11.1%	3.9	4.2 ± 3.8	29.6%	3.2	10.9 ± 6.5
T Complex	0.0%	4.3	NA	**14.8%**	**3.6**	**8.3 ± 7.1**	**40.7%**	**2.9**	**6.8 ± 5.5**
ST I	**14.8%**	**4.2**	**6.1 ± 5.2**	**29.6%**	**3.7**	**9.3 ± 7.3**	**51.9%**	**3.0**	**8.4 ± 8.0**
ST II	0.0%	5.3	NA	0.0%	4.4	NA	18.5%	3.3	6.8 ± 5.1
ST V	3.7%	5.2	0.4 ± 0.0	7.4%	4.1	7.3 ± 9.8	33.3%	3.1	10.5 ± 6.5
SDNN	**11.1%**	**4.7**	**6.3 ± 6.0**	**14.8%**	**4.2**	**8.7 ± 7.4**	**40.7%**	**3.6**	**11.0 ± 8.6**
HRV total	**11.1%**	**4.0**	**5.8 ± 5.2**	**18.5%**	**3.8**	**8.6 ± 7.2**	25.9%	3.0	7.5 ± 8.1
HRV VLF	0.0%	5.4	NA	0.0%	4.9	NA	3.7%	3.5	3.7 ± 0.0
HRV LF	3.7%	4.9	15.8 ± 0.0	3.7%	4.7	15.8 ± 0.0	11.1%	4.0	10.4 ± 7.8
HRV HF	7.4%	6.0	5.7 ± 3.4	7.4%	5.5	5.7 ± 3.4	14.8%	4.4	7.1 ± 6.6
HRV Norm LF	0.0%	4.9	NA	7.4%	4.1	8.7 ± 9.1	14.8%	2.8	8.3 ± 5.4
HRV Norm HF	3.7%	5.2	9.6 ± 0.0	7.4%	4.7	6.8 ± 4.0	18.5%	4.1	9.0 ± 5.9

Physiol Meas. Author manuscript; available in PMC 2016 December 01.

Table 3

List of true positive rate (TPR) achievable under a prescribed maximal false positive rate (FPR) for the terminal value alarm of each ECG metric (27 case patients).

		max FPR = 0.00			max FPR = 0.01			max FPR = 0.05		
		TPR	**Threshold**	**Lead Time (hours)**	**TPR**	**Threshold**	**Lead Time (hours)**	**TPR**	**Threshold**	**Lead Time (hours)**
PR	+	0.0%	366 ms	NA	0.0%	298 ms	NA	0.0%	232 ms	NA
	−	0.0%	94 ms	NA	0.0%	100 ms	NA	0.0%	115 ms	NA
Pdur	+	0.0%	172 ms	NA	3.7%	164 ms	0.4 ± 0.0	3.7%	145 ms	0.4 ± 0.0
	−	0.0%	32 ms	NA	0.0%	67 ms	NA	0.0%	79 ms	NA
QRSdur	+	0.0%	246 ms	NA	0.0%	215 ms	NA	3.7%	182 ms	15.3 ± 0.0
	−	0.0%	22 ms	NA	3.7%	70 ms	11.0 ± 0.0	3.7%	76 ms	11.0 ± 0.0
RR	+	3.7%	1313 ms	0.03 ± 0.0	3.7%	1163 ms	0.03 ± 0.0	7.4%	978 ms	7.4 ± 10.4
	−	0.0%	384 ms	NA	7.4%	451 ms	1.6 ± 0.3	14.8%	514 ms	4.1 ± 3.7
QT	+	3.7%	600 ms	4.1 ± 0.0	3.7%	574 ms	4.1 ± 0.0	11.1	492 ms	1.4 ± 2.4
	−	0.0%	162 ms	NA	0.0%	241 ms	NA	11.1%	313 ms	1.5 ± 0.4
SerumK2	+	0.0%	8.5 mM	NA	0.0%	8.0 mM	NA	0.0%	6.6 mM	NA
	−	0.0%	0.1 mM	NA	0.0%	0.5 mM	NA	3.7%	1.6 mM	1.9 ± 0.0
T Complex	+	0.0%	1.0	NA	0.0%	0.8	NA	7.4%	0.6	0.2 ± 0.3
	−	0.0%	0.01	NA	0.0%	0.03	NA	7.4%	0.05	15.4 ± 7.4
ST I	+	0.0%	549 μV	NA	0.0%	220 μV	NA	3.7%	105 μV	2.4 ± 0.0
	−	0.0%	−179 μV	NA	7.4%	−122 μV	18.6 ± 1.5	22.2%	−56 μV	12.8 ± 8.3
ST II	+	3.7%	414 μV	10.4 ± 0.0	3.7%	240 μV	10.4 ± 0.0	7.4%	143 μV	16.1 ± 8.1
	−	0.0%	−775 μV	NA	0.0%	−151 μV	NA	0.0%	−75 μV	NA
ST V	+	0.0%	555 μV	NA	3.7%	291 μV	4.0 ± 0.0	7.4%	166 μV	10.8 ± 9.6
	−	3.7%	−321 μV	0.4 ± 0.0	7.4%	−232 μV	3.7 ± 4.7	7.4%	−87 μV	3.7 ± 4.7
SDNN	+	0.0%	167 ms	NA	3.7%	136 ms	15.8 ± 0.0	3.7%	121 ms	15.8 ± 0.0
	−	3.7%	3 ms	4.1 ± 0.0	7.4%	5 ms	10.6 ± 9.2	11.1%	6 ms	12.0 ± 6.9
HRV total	+	0.0%	1.7×10^4 ms^2	NA	0.0%	1.6×10^4 ms^2	NA	3.7%	1.3×10^4 ms^2	9.7 ± 0.0
	−	3.7%	14 ms^2	4.2 ± 0.0	11.1%	43 ms^2	10.3 ± 8.7	18.5%	77 ms^2	9.4 ± 7.9

		max FPR = 0.00			max FPR = 0.01			max FPR = 0.05		
		TPR	**Threshold**	**Lead Time (hours)**	**TPR**	**Threshold**	**Lead Time (hours)**	**TPR**	**Threshold**	**Lead Time (hours)**
HRV VLF	+	0.0%	2.3×10^3 ms^2	NA	0.0%	2.2×10^3 ms^2	NA	0.0%	1.9×10^3 ms^2	NA
	−	0.0%	3.1 ms^2	NA	0.0%	3.8 ms^2	NA	0.0%	4.5 ms^2	NA
HRV LF	+	0.0%	3.0×10^3 ms^2	NA	0.0%	2.7×10^3 ms^2	NA	7.4%	2.1×10^3 ms^2	6.9 ± 7.0
	−	0.0%	1.8 ms^2	NA	0.0%	2.4 ms^2	NA	3.7%	3.1 ms^2	2.1 ± 0.0
HRV HF	+	0.0%	1.5×10^4 ms^2	NA	0.0%	1.2×10^4 ms^2	NA	3.7%	1.0×10^4 ms^2	3.3 ± 0.0
	−	3.7%	3.0 ms^2	9.6 ± 0.0	7.4%	4.2 ms^2	10.8 ± 1.7	14.8%	9.8 ms^2	14.9 ± 4.9
HRV norm LF	+	0.0%	62%	NA	0.0%	57%	NA	0.0%	45%	NA
	−	0.0%	5.3%	NA	0.0%	6.4%	NA	3.7%	8.0%	16.3 ± 0.0
HRV norm HF	+	0.0%	62%	NA	0.0%	59%	NA	3.7%	52%	14.4 ± 0.0
	−	3.1%	11%	8.0 ± 0.0	3.1%	13%	8.0 ± 0.0	11.1%	17%	7.4 ± 2.9

Physiol Meas. Author manuscript; available in PMC 2016 December 01.

Table 4

List of true positive rate (TPR) achievable under a prescribed maximal false positive rate (FPR) for the slope alarm of each ECG metric (27 case patients).

		max FPR = 0.00			max FPR = 0.01			max FPR = 0.05		
		TPR	**Threshold**	**Lead Time (hours)**	**TPR**	**Threshold**	**Lead Time (hours)**	**TPR**	**Threshold**	**Lead Time (hours)**
PR	+	0.0%	84.8 ms/hour	NA	0.0%	60.0 ms/hour	NA	18.5%	17.5 ms/hour	9.9 ± 6.6
	−	3.7%	−48.9 ms/hour	22.2 ± 0.0	3.7%	−26.5 ms/hour	22.2 ± 0.0	18.5%	−8.8 ms/hour	8.4 ± 10.2
Pdur	+	0.0%	85.3 ms/hour	NA	0.0%	35.8 ms/hour	NA	11.1%	11.7 ms/hour	6.3 ± 10.2
	−	0.0%	−50.7 ms/hour	NA	0.0%	−37.3 ms/hour	NA	0.0%	−18.7 ms/hour	NA
QRSdur	+	0.0%	59.4 ms/hour	NA	3.7%	17.8 ms/hour	17.7 ± 0.0	14.8%	7.4 ms/hour	7.2 ± 7.6
	−	0.0%	−183.7 ms/hour	NA	0.0%	−41.9 ms/hour	NA	3.7%	−11.3 ms/hour	13.3 ± 0.0
RR	+	7.4%	69.0 ms/hour	9.8 ± 4.8	7.4%	57.5 ms/hour	9.8 ± 4.8	14.8%	45.7 ms/hour	5.8 ± 5.6
	−	0.0%	−148.9 ms/hour	NA	0.0%	−125.5 ms/hour	NA	0.0%	−66.6 ms/hour	NA
QT	+	**11.1%**	**29.6 ms/hour**	**10.4 ± 7.9**	**22.2%**	**23.0 ms/hour**	**7.8 ± 6.8**	25.9%	19.4 ms/hour	6.7 ± 6.9
	−	7.4%	−54.6 ms/hour	0.1 ± 0.1	7.4%	−45.8 ms/hour	0.1 ± 0.1	11.1%	−23.5 ms/hour	7.3 ± 12.5
SerumK2	+	0.0%	2.9 mM/hour	NA	3.7%	1.8 mM/hour	10.6 ± 0.0	7.4%	1.0 mM/hour	5.3 ± 7.5
	−	0.0%	−2.4 mM/hour	NA	0.0%	−2.1 mV/hour	NA	3.7%	−0.9 mM/hour	9.1 ± 0.0
T Complex	+	0.0%	0.4 /hour	NA	0.0%	0.2 /hour	NA	14.8%	0.1 /hour	4.2 ± 6.4
	−	0.0%	−0.3 /hour	NA	3.7%	−0.14 /hour	2.0 ± 0.0	3.7%	−0.1 /hour	2.0 ± 0.0
ST I	+	3.7%	43.0 μV/hour	19.6 ± 0.0	7.4%	21.9 μV/hour	11.0 ± 12.2	14.8%	8.8 μV/hour	6.0 ± 9.1
	−	0.0%	−82.2 μV/hour	NA	0.0%	−69.4 μV/hour	NA	7.4%	−24.2 μV/hour	13.2 ± 11.7
ST II	+	0.0%	66.4 μV/hour	NA	3.7%	53.5 μV/hour	4.7 ± 0.0	14.8%	37.6 μV/hour	3.2 ± 1.3
	−	0.0%	−39.8 μV/hour	NA	7.4%	−30.8 μV/hour	6.3 ± 8.5	14.8%	−14.6 μV/hour	10.1 ± 8.5
ST V	+	7.4%	67.6 μV/hour	0.6 ± 0.7	7.4%	64.9 μV/hour	0.6 ± 0.7	14.8%	32.6 μV/hour	5.4 ± 9.5
	−	0.0%	−87.8 μV/hour	NA	0.0%	−58.5 μV/hour	NA	3.7%	−29.4 μV/hour	0.4 ± 0.0
SDNN	+	0.0%	890 ms/hour	NA	0.0%	863 ms/hour	NA	0.0%	832 ms/hour	NA
	−	0.0%	−387 ms/hour	NA	3.7%	−332 ms/hour	9.7 ± 0.0	3.7%	−278 ms/hour	9.7 ± 0.0
HRV total	+	0.0%	9.2×10^4 ms^2/hour	NA	3.7%	8.3×10^4 ms^2/hour	16.4 ± 0.0	7.4%	5.0×10^4 ms^2/hour	12.2 ± 5.9
	−	3.7%	-3.0×10^4 ms^2/hour	5.8 ± 0.0	3.7%	-2.3×10^4 ms^2/hour	5.8 ± 0.0	11.1%	-1.1×10^4 ms^2/hour	7.9 ± 2.9
HRV VLF	+	0.0%	2.0×10^4 ms^2/hour	NA	0.0%	1.7×10^4 ms^2/hour	NA	3.7%	1.1×10^4 ms^2/hour	2.4 ± 0.0

		max FPR = 0.00			max FPR = 0.01			max FPR = 0.05		
		TPR	**Threshold**	**Lead Time (hours)**	**TPR**	**Threshold**	**Lead Time (hours)**	**TPR**	**Threshold**	**Lead Time (hours)**
	−	0.0%	-5.3×10^4 ms^2/hour	NA	0.0%	-4.9×10^4 ms^2/hour	NA	0.0%	-4.0×10^4 ms^2/hour	NA
HRV LF	+	0.0%	2.5×10^4 ms^2/hour	NA	7.4%	1.8×10^4 ms^2/hour	6.3 ± 4.5	7.4%	1.7×10^4 ms^2/hour	6.3 ± 4.5
	−	0.0%	-6.0×10^4 ms^2/hour	NA	0.0%	-5.7×10^4 ms^2/hour	NA	3.7%	-5.3×10^4 ms^2/hour	7.7 ± 0.0
HRV HF	+	0.0%	1.8×10^5 ms^2/hour	NA	0.0%	1.7×10^5 ms^2/hour	NA	3.7%	1.6×10^5 ms^2/hour	9.5 ± 0.0
	−	3.7%	-1.9×10^5 ms^2/hour	14.7 ± 0.0	7.4%	-1.3×10^5 ms^2/hour	12.0 ± 3.9	7.4%	$-1.0-10^5$ ms^2/hour	12.0 ± 3.9
HRV norm LF	+	0.0%	689% /hour	NA	3.7%	640% /hour	3.3 ± 0.0	3.7%	512% /hour	3.3 ± 0.0
	−	3.7%	−311% /hour	5.4 ± 0.0	3.7%	−293% /hour	5.4 ± 0.0	3.7%	−262% /hour	5.4 ± 0.0
HRV norm HF	+	3.7%	264% /hour	7.9 ± 0.0	7.4%	252% /hour	10.0 ± 3.0	7.4%	219% /hour	10.0 ± 3.0
	−	0.0%	−2021% /hour	NA	0.0%	974% /hour	NA	11.1%	312% /hour	11.9 ± 7.5

Table 5

The highest achievable TPRs with zero FPR by performing the "OR" logic on 2, 3, and 4 zero-FPR alarm conditions. The combined alarm conditions with the highest achievable TPR are all based on the trend duration alarms.

Number of alarms combined by the "OR" logic	Highest achievable TPR with zero FPR	Combined alarm conditions (all based on the trend duration alarms)
2	22.2%	PR, ST I RR, ST I SerumK2, ST I
3	29.6%	RR, SerumK2, ST I
4	33.3%	RR, QRSdur, SerumK2, ST I RR, SDNN, SerumK2, ST I